American Mineralogist, Volume 60, pages 398–406, 1975

The System Mg_2SiO_4–SiO_2 at Pressures Up to 25 Kilobars[1]

CHENG-HONG CHEN,[2] AND DEAN C. PRESNALL

Institute for Geological Sciences, University of Texas at Dallas
P. O. Box 688, Richardson, Texas 75080

Abstract

Using piston-cylinder apparatus, two univariant solidus curves involving the phases forsterite + enstatite + liquid and enstatite + silica + liquid have been bracketed at pressures up to 25 kbar. Also, the protoenstatite-orthoenstatite inversion curve has been reversed at 8 kbar and 1313° to 1417°C. Three invariant points have been located. One involves the phases forsterite, protoenstatite, orthoenstatite, and liquid and is located at 15.2 kbar, 1700°C. The second involves the phases high quartz, protoenstatite, orthoenstatite, and liquid and is located at 15.6 kbar, 1720°C. The third involves protoenstatite, orthoenstatite, and liquid and is placed at 15.8 kbar, 1730°C. A fourth invariant point involving the phases cristobalite, high quartz, protoenstatite, and liquid has not been bracketed closely but occurs approximately at 4.1 kbar, 1620°C. The composition of the isobaric eutectic between silica and enstatite does not change measurably with pressure at least up to 25 kbar. The one-atmosphere peritectic liquid in equilibrium with forsterite and enstatite changes to a eutectic liquid at a pressure of approximately 1.3 kbar and its composition moves progressively toward forsterite as pressure increases. However, this result for the binary system does not necessarily mean that the reaction relation involving forsterite, enstatite, and liquid in a natural magma must disappear at a similar pressure.

Introduction

In 1914, Bowen and Andersen published their classic results on melting relations in the system MgO–SiO_2 at one atmosphere pressure. Their discovery of the incongruent melting relationship of enstatite to form forsterite and liquid has occupied a central position in the development of petrogenetic theory to the present day. Phase relations in this system at higher pressures are known only in part. Davis and England (1964) determined the melting curve of forsterite up to 47 kbar. Boyd, England, and Davis (1964) studied the melting behavior of enstatite up to 47 kbar and found that the incongruent melting relationship of enstatite disappears at some pressure less than 5.4 kbar. Taylor (1973) located the position of the eutectic between forsterite and enstatite at 15 kbar. The polymorphism of enstatite at high pressures has been studied by Boyd *et al* (1964), Kushiro, Yoder, and Nishikawa (1968), and Anastasiou and Seifert (1972).

The purpose of this paper is to present the phase relations for the system Mg_2SiO_4–SiO_2 over the pressure range of 1 atm to 25 kbar. Two univariant solidus curves in *P-T* space have been determined, one involving forsterite, enstatite, and liquid, and the other involving enstatite, silica, and liquid. In addition, we have studied the protoenstatite-orthoenstatite inversion at subsolidus temperatures and have obtained new data bearing on the discrepancy in the position of this transition determined by Boyd *et al* (1964) *versus* that determined by Kushiro *et al* (1968) and Anastasiou and Seifert (1972).

Experimental Method

Experiments at 1 atmosphere pressure were carried out in a standard platinum-wound vertical quench furnace, and high pressure experiments were carried out with a piston-cylinder apparatus (Boyd and England, 1960). All high pressure experiments were of the decompression or piston-out type, and no pressure correction was applied. Platinum sample capsules were used together with the pressure cell arrangement described by Presnall, Brenner, and

[1] Contribution No. 269, Institute for Geological Sciences, University of Texas at Dallas.

[2] Present address: Department of Geology, National Taiwan University, Taipei, Taiwan, R. O. C.

O'Donnell (1973). Pt/Pt10Rh thermocouples, used for experiments at one atmosphere, were calibrated by comparison against a standard Pt/Pt10Rh thermocouple calibrated by the National Bureau of Standards. W3Re/W25Re thermocouples, used for high pressure experiments, were calibrated by Engelhard Industries, Inc., to a stated uncertainty of ±10°C. All temperatures were corrected to conform to the 1968 International Practical Temperature Scale (IPTS-68) (anonymous, 1969). No pressure correction was applied to the temperature readings. Two starting compositions were prepared: one at 56.44% SiO_2, 43.56% MgO by weight (composition A, Fig. 1); and the other at 65.07% SiO_2, 34.93% MgO (composition B, Fig. 1). The source of MgO and SiO_2 for these mixtures is the same as described earlier (Presnall, Simmons, and Porath, 1972). Both mixtures were fired in a gas furnace for four hours, composition A at about 1700°C and composition B at about 1660°C. The mixtures were quenched in water to a combination of glass and quench crystals. For the high pressure experiments, all parts of the pressure cell within and including the boron nitride sleeve (except the thermocouple) were fired for one hour at 1050°C prior to assembly. The W3Re/W25Re thermocouple was dried for one hour at 70°C. Polished thin sections of runs bracketing univariant *P-T* lines were made for examination in both transmitted and reflected light, and in some cases for determination of glass composition with an electron microprobe (Applied Research Laboratories, Model EMX-SM). The raw microprobe data were corrected for fluorescence, absorption, and atomic number effects using the EMPADR VII computer program of Rucklidge and Gasparrini (1969).

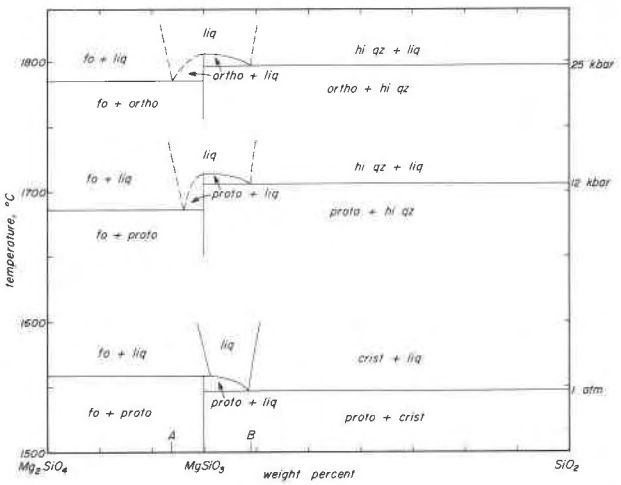

FIG. 1. Temperature-composition sections for the system Mg_2SiO_4–SiO_2 at 1 atm, 12 kbar, and 25 kbar. Compositions A and B are the two starting mixtures used in this study.

Melting Relations at One Atmosphere Pressure

Although we had no reason to doubt the original work of Bowen and Andersen (1914) on the system MgO–SiO_2 at one atmosphere, their diagram has not been reexamined for 60 years. Thus, we decided to check some critical parts of the phase diagram.

Table 1 shows our quenching results at one atmosphere, and the phase diagram is shown at the bottom of Figure 1. We have determined the incongruent melting temperature of enstatite to be 1559°C; Bowen and Andersen found this temperature to be 1557°C, which when corrected to IPTS-69, is 1562°C. These two results are identical within the experimental uncertainty. The composition of the liquid at this peritectic point, determined with an electron microprobe, is 60.6 percent SiO_2, which also agrees with the value of 60.9 percent SiO_2 obtained by Bowen and Andersen. We have found the temperature for the eutectic between enstatite and cristobalite to be 1547°C, which agrees exactly with the value given by Bowen and Andersen when corrected to IPTS-68. Mixture B (65.07 percent SiO_2) contains slightly more silica than the eutectic composition (65.0 percent SiO_2) found by Bowen and Andersen. We observed a small melting interval (about 12°C) with cristobalite as the primary phase, a result in agreement with Bowen and Andersen's location for the eutectic. In summary, we have found complete agreement with the original work of Bowen and Andersen (1914).

Protoenstatite-Orthoenstatite Inversion

Anastasiou and Seifert (1972), in good agreement with Kushiro *et al* (1968), bracketed the protoenstatite-orthoenstatite inversion curve from one atmosphere, 985°C (Atlas, 1952) up to 8 kbar, 1355°C. However, linear extrapolation of their curve to higher temperatures and pressures is in sharp disagreement with the earlier high-temperature results of Boyd *et al* (1964). In an attempt to resolve this discrepancy, we have studied the inversion from about 1290° to 1690°C. Our experiments thus overlap the entire temperature range studied by Boyd *et al* (1964) and the upper part of the temperature range studied by Kushiro *et al* (1968) and Anastasiou and Seifert (1972).

Our subsolidus quenching results are listed in Table 2. Phases present were determined from X-ray

TABLE 1. Quenching Results for Near-Solidus Experiments

Composition A (56.44 % SiO_2, 43.56 % MgO by wt.)				Composition B (65.07 % SiO_2, 34.93 % MgO by wt.)			
T (°C)	P (kbar)	Time (hr)	Phases Present*	T (°C)	P (kbar)	Time (hr)	Phases Present*
1554	1 atm	6	en + fo	1545	1 atm	6	en + crist
1559	1 atm	9	en + fo + gl + q	1547	1 atm	6	en + crist + gl + q
1564	1 atm	10	fo + gl	1551	1 atm	6	crist + gl
1634	7	4	en + fo + gl + q	1555	1 atm	10	crist + gl
1639	7	4	fo + gl + q	1562	1 atm	8	gl
1645	7	4	fo + gl + q	1665	7	4	en + qz
1639	10	0.25	ortho** + fo	1678	7	4	gl
1650	10	4	en + fo	1680	7	4	en + qz + gl + q
1665	10	4	en + fo + gl + q	1681	7	4	en + qz
1686	10	4	fo + gl	1691	7	4	gl
1696	10	0.25	fo + gl + q	1696	10	4	en + qz
1676	15	4	en + fo	1714	10	4	gl
1701	15	4	en + fo + gl + q	1714	15	4	en + qz + gl + q
1728	15	4	fo + gl + q	1728	15	4	gl + q
1749	15	4	fo + gl + q	1728	15	3	en + qz + gl + q
1739	16	0.25	fo + gl + q	1759	20	3	en + qz
1676	20	3	en + fo	1770	20	3	gl + q
1749	20	2	en + fo + gl + q	1790	25	2	en + qz + gl + q
1770	20	1.5	en + fo + gl + q				
1770	25	2	en + fo				
1790	25	2	en + fo + gl + q				
1811	25	2	gl + q				

*en = enstatite; ortho = orthoenstatite; crist = cristobalite; qz = quartz; fo = forsterite; gl = glass; q = quench crystals. Twinned enstatite (interpreted to be clinoenstatite inverted from protoenstatite during quenching) was observed in runs at 7 kbar but was not found at higher pressures.
**Determined by X-ray powder diffraction.

powder diffraction patterns, using for reference the X-ray data given by Atlas (1952) and Borg and Smith (1969). Figure 2 shows a comparison of our quenching data with the curves of Boyd *et al* (1964), Kushiro *et al* (1968), and Anastasiou and Seifert (1972). Following Atlas (1952) and Smyth (1974), we have assumed that the presence of clinoenstatite is the result of inversion of protoenstatite on quenching. With this assumption, our data at 7 kbar and at temperatures below 1450°C at higher pressures agree with the curve of Kushiro *et al* (1968) and Anastasiou and Seifert (1972).

At 8 kbar we achieved a reversal of the phase boundary. For each reversal run (see Table 3), the sample was held initially on one side of the curve for a time sufficient to produce the one phase assemblage. The temperature was then changed and held on the other side of the curve. The phases produced at the end of the initial conditions were determined from separate runs (see Table 2). Within the limits of detectability of the X-ray diffractometer, the reaction of orthoenstatite to protoenstatite went to completion. The reverse reaction from protoenstatite to orthoenstatite did not quite go to completion, but the reversal is considered valid because a large amount of orthoenstatite was produced.

As shown in Figure 2, most of our data above 1450°C and 7 kbar do not agree with the curve of Anastasiou and Seifert (1972) and Kushiro *et al* (1968), nor with our own data at lower pressures and temperatures. Orthoenstatite was observed in what we expected to be the protoenstatite field. Interestingly, two runs listed by Kushiro *et al* (1968) at 10 kbar (1500° and 1525°C) showed orthoenstatite, in agreement with our results but in disagreement with the position of their inversion curve. Another interesting feature is that if we had made runs only in the temperature range above 1550°C studied by Boyd *et al* (1964), we would have agreed with the position of the curve determined by them.

We believe the reversal achieved at 8 kbar strongly supports the location of the curve as determined by

TABLE 2. Subsolidus Quenching Results for Starting Composition B (65.07 % SiO_2, 34.93 % MgO by weight)

T (°C)	P (kbar)	Time (hr)	Phases Present*
1292	7	4	ortho
1344	7	2	clino + proto
1417	7	2	clino + proto
1520	7	2	clino + proto
1645	7	4	clino + proto
1313	8	2	ortho
1334	8	2	clino + proto + ortho
1417	8	2	clino + proto
1417	8	13	clino + proto
1624	8	2	ortho
1520	8.4	2	ortho
1417	9	2	clino + proto + ortho
1437	9	2	clino + proto + ortho
1624	9	2	ortho
1437	10	2	ortho
1500	10	2	ortho
1500	10	12	ortho
1624	10	2	ortho
1666	10	4	ortho
1686	13	4	ortho
1686	16	4	ortho

*ortho = orthoenstatite; clino = low clinoenstatite; proto = protoenstatite. Quartz is universally present.

Kushiro *et al* (1968) and Anastasiou and Seifert (1972). The higher pressure, higher temperature runs can be explained if it is assumed that for these runs protoenstatite inverted directly to orthoenstatite during quenching. At low pressures, there appears to be agreement that protoenstatite inverts during quenching either partially or completely to clinoenstatite. However, at higher pressures, the protoenstatite to orthoenstatite inversion occurs at much higher temperatures and may make direct conversion of protoenstatite to orthoenstatite possible during quenching. For the quenching rates applicable to our piston-cylinder apparatus, this interpretation implies that protoenstatite inverts partially to clinoenstatite when the protoenstatite-to-orthoenstatite curve lies below about 1300°C (below 7 kbar). However, when this curve lies above about 1450°C (above 10 kbar), protoenstatite inverts directly to orthoenstatite. The temperature range 1300 to 1450°C is transitional and shows both types of behavior.

However, this is not the only possible explanation. Smyth (1974) has found that for slow cooling rates at one atm pressure, protoenstatite transforms initially to clinoenstatite and then to orthoenstatite. At higher pressures, this sequence of events may also occur but much more rapidly, so that no trace of protoenstatite or clinoenstatite remains after quenching. Also, Smyth worked on single crystals whereas we have studied much finer grained material. This could cause a difference in nucleation rates.

In any case, we prefer the position of the protoenstatite-orthoenstatite curve as determined by Kushiro *et al* (1968) and Anastasiou and Seifert (1972), and we base this preference on the reversal we have obtained at 8 kbar. Further clarification of the equilibrium relations might be obtainable from examination of quenched samples by high resolution electron microscopy (Buseck and Iijima, 1974), or from an X-ray study at high temperatures and pressures.

Solidus Phase Relations at High Pressures

The isopleth for the composition 43.56% MgO, 56.44% SiO_2 (composition A, Fig. 1) is shown in Figure 3, and the quenching results are listed in Table 1. The solidus has been bracketed up to 25 kbar and consists of two univariant curves, one involving forsterite, protoenstatite, and liquid at low pressures, and the other involving forsterite, orthoenstatite, and liquid at high pressures. The invariant point i_1 is placed at 15.2 kbar, 1700°C, based on a linear extrapolation of the preferred protoenstatite-orthoenstatite inversion curve from Figure 2. The liquidus curve (dashed) approaches the solidus curve as pressure in-

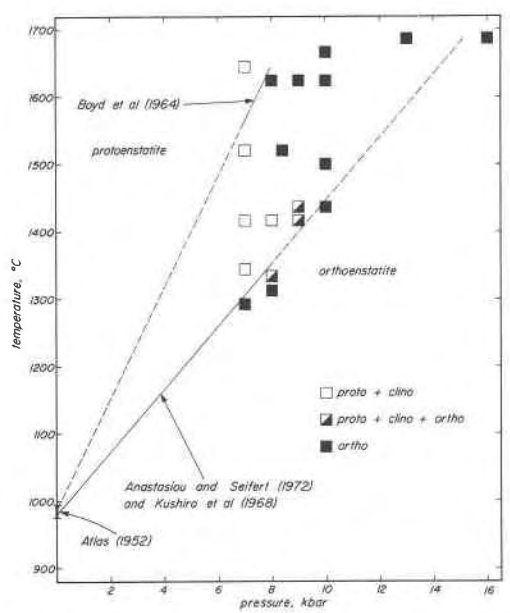

FIG. 2. Subsolidus experiments on mixture B. Quartz is always present in addition to the phases indicated.

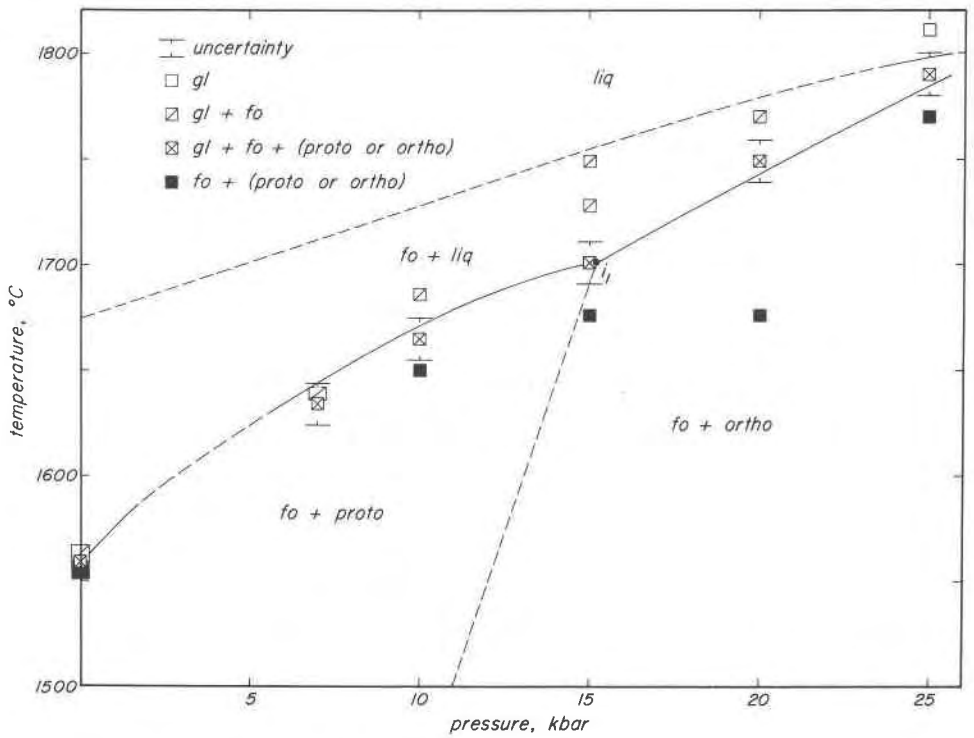

FIG. 3. Isopleth for the composition 43.56 percent MgO, 56.44 percent SiO_2 by weight (mixture A).

creases, and extrapolation to higher pressures suggests the two curves touch at about 27 kbar. This shows that the liquid composition in equilibrium with forsterite and enstatite moves continuously toward forsterite as pressure increases and would coincide with the composition of our starting mixture at about 27 kbar. The temperature we have obtained for the eutectic between orthoenstatite and forsterite at 15 kbar is 1700°C, in close agreement with the value of 1710°C found by Taylor (1973).

Figure 4 shows the isopleth for the composition 34.93% MgO, 65.07% SiO_2 (composition B, Fig. 1). Again, the solidus curve has been determined, and it consists of three univariant lines. At low pressures (below i_4) the phases in equilibrium along the solidus curve are cristobalite, protoenstatite, and liquid; at intermediate pressures (between i_4 and i_2) the phases are high quartz, protoenstatite, and liquid; and at high pressures (above i_2) the phases are high quartz, orthoenstatite, and liquid. As in Figure 3, the location of invariant point i_2 is based on a linear extrapolation of the preferred protoenstatite-orthoenstatite inversion curve in Figure 2 and is placed at 15.6 kbar, 1720°C. The location of invariant point i_4 (4.1 kbar, 1620°C) is only approximate and is based on the inferred location of the cristobalite-high quartz inversion curve given by Tuttle and Bowen (1958, p. 29).

As mentioned earlier, the starting composition was made up with a very slight excess of SiO_2 over that in the one-atmosphere eutectic of Bowen and Andersen (1914). Although a very small field of cristobalite + liquid was detected at one atmosphere pressure, no melting interval was found in the high pressure experiments, indicating that throughout the pressure range studied, the composition of the eutectic liquid remains essentially constant and equal to the composition of the starting mixture (34.93% MgO, 65.07% SiO_2). In one run at 15 kbar and another at 25 kbar, part of the capsule contained glass or glass plus quench crystals and the other part contained quartz plus enstatite. Thus, these runs were located exactly on the univariant curve. In both runs, microprobe area scan analysis of the portion containing glass or glass plus quench crystals gave the same composition as the starting composition, thus confirming the lack of change of the eutectic liquid composition with pressure.

In order to establish times required for equilibrium, each of the univariant solidus curves in Figures 3 and 4 was reversed at one pressure above (16 kbar) and one pressure below (10 kbar) the in-

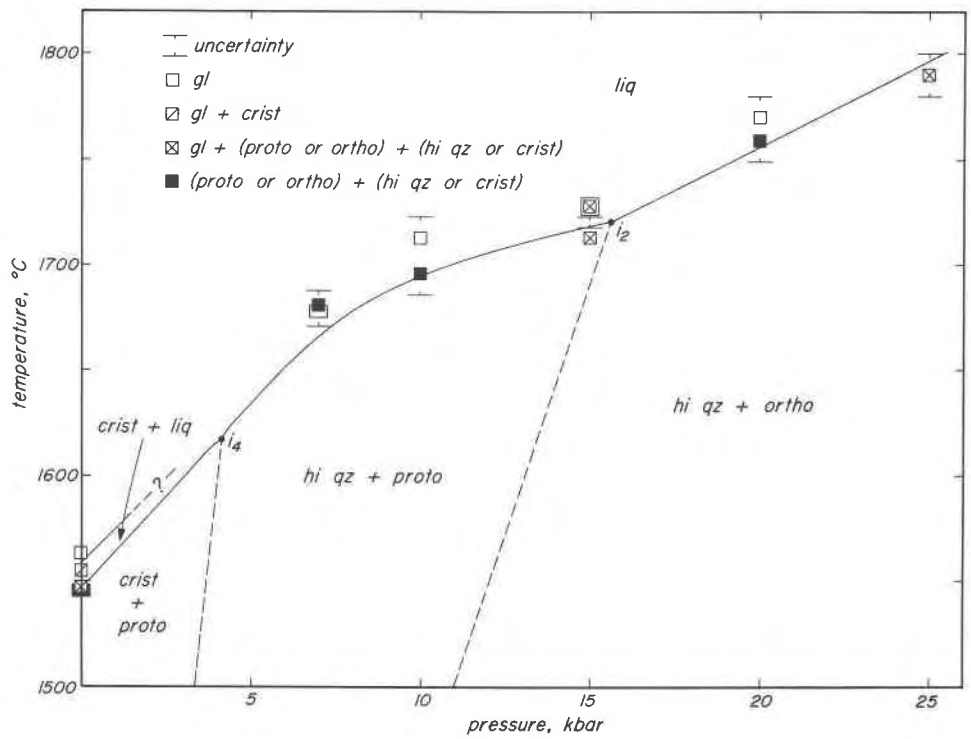

FIG. 4. Isopleth for the composition 34.93 percent MgO, 65.07 percent SiO_2 by weight (mixture B).

variant points i_1 and i_2 (Table 3). These run times were then used as a guide in making bracketing runs at other points on the curves (Table 1). As indicated in Table 3, some of the reversal runs were quenched after the initial conditions and the sample placed in a new platinum capsule for the final conditions. This was done because a single long run would have risked melting the platinum capsule (Presnall *et al,* 1973).

Figure 5 shows the *P-T* projection of the system Mg_2SiO_4–SiO_2. At pressures below 15 kbar we have raised the temperature of the melting curve of orthoenstatite (protoenstatite on our diagram) given by Boyd *et al* (1964) in order to keep it higher than our curve for the eutectic between protoenstatite and high quartz. This new location for the protoenstatite melting curve lies about 15°C above the 5.4 and 8.3 kbar uncertainty brackets of Boyd *et al* (1964). At all other pressures, our position for the enstatite melting curve lies within their uncertainty brackets. Invariant point i_3 lying on the enstatite melting curve involves protoenstatite, orthoenstatite, and liquid, and is placed at 15.8 kbar, 1730°C. The exact location of the singular point *s*, at which protoenstatite begins to melt congruently, has not been determined, but extrapolation of the curve for the eutectic between protoenstatite and forsterite (line s-i_1) suggests that the singular point is located at a pressure of about 1.3 kbar, slightly lower than the pressure of 2.3 kbar calculated by Boyd *et al* (1964).

Figure 1 shows temperature-composition sections at 1 atm, 12 kbar, and 25 kbar. These illustrate two features of the phase relations already discussed. That is, the composition of the eutectic between enstatite and quartz remains essentially constant at all pressures, and the composition of the liquid in

TABLE 3. Quenching Results for Reversal Runs

Initial Conditions			Final Conditions			
T (°C)	P (kbar)	Time (hr)	T (°C)	P (kbar)	Time (hr)	Phases Present*
Composition A (56.44 % SiO_2, 43.56 % MgO by wt.)						
1639	10	0.25	1696	10	3	fo + gl + q
1696	10	0.25	1639	10	4	fo + en
1676	16	4	1739	16	1.5	fo + gl + q**
1739	16	0.25	1676	16	1.5	fo + en + q
Composition B (65.07 % SiO_2, 34.93 % MgO by wt.)						
1313	8	2	1417	8	2	proto + clino + qz
1417	8	2	1313	8	4	ortho + clino + qz
1666	10	4	1739	10	3	en + qz + gl + q**
1739	10	3	1666	10	3	en + qz**
1686	16	4	1749	16	2	gl**
1749	16	2	1686	16	2	en + qz**

*Abbreviations same as in Tables 1 and 2.
**The sample was quenched after the initial conditions and a new Pt capsule was used for the final conditions.

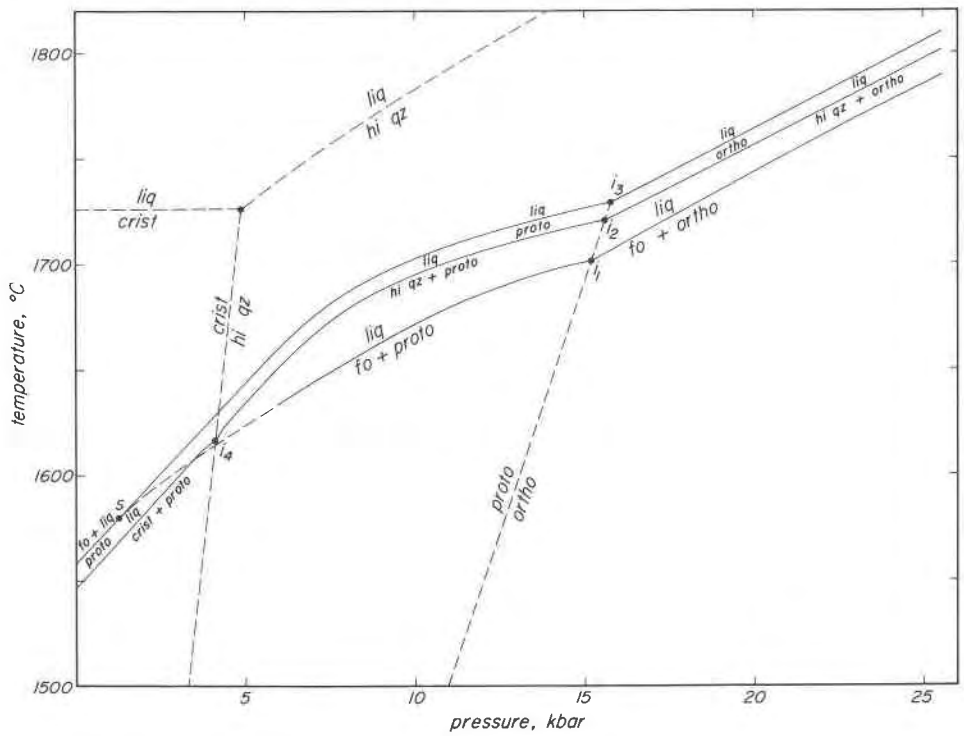

FIG. 5. Pressure-temperature projection for the system Mg_2SiO_4–SiO_2 showing univariant lines (dashed where inferred) and invariant points. The point *s* is a singular point.

equilibrium with forsterite and enstatite moves continuously toward forsterite as pressure increases. The position of the eutectics between forsterite and enstatite at 12 and 25 kbar are approximate and are based on interpolation between three points: Taylor's (1973) determination at 15 kbar, the assumption that the singular point *s* (Fig. 5) occurs at 1.3 kbar, and our extrapolated location of 56.4% SiO_2, 43.6% MgO at about 27 kbar.

Geologic Discussion

An important cornerstone of Bowen's scheme for the production of various igneous rock types by fractional crystallization of basaltic magma (Bowen, 1928) is the incongruent melting of enstatite to produce forsterite and liquid. This reaction, he argued, could produce silica-saturated magmas by fractional crystallization of silica-undersaturated magmas. Our data fit best with the disappearance of this reaction at about 1.3 kbar. However, it should not be inferred from our data for the binary system that the reaction relation in natural magmas also disappears at a similar pressure. It has long been known that, at one atmosphere, the presence of iron causes the reaction relation to disappear (Bowen and Schairer, 1935). Taylor (1973) has found that at 15 kbar the presence of aluminum in enstatite has the opposite effect. That is, the reaction occurs for aluminous enstatite but does not if aluminum is absent. If another phase such as spinel is present, the matter is even more complicated. That is, it is possible for the reaction to occur in the presence of an extra phase but not in its absence. In this regard, it is noteworthy that in some volcanic rocks (for example, see Kuno, 1950) olivine phenocrysts are encased by composite reaction rims containing both orthopyroxene and spinel. Thus, we disagree with the conclusion of Boyd *et al* (1964, p. 2107) that the reaction relation between olivine and enstatite in natural magmas must necessarily be confined to near-surface fractionation processes. The matter is still unresolved.

Kushiro (1968) showed that in several anhydrous systems approximating mantle chemistry, increasing pressure causes primary melts to become increasingly depleted in silica. In the system Mg_2SiO_4–SiO_2, the composition best approximating a peridotitic mantle would be slightly toward enstatite from forsterite. Figure 1 shows that such a mantle would produce increasingly silica-depleted primary magmas as pressure is increased, in agreement with Kushiro's

(1968) results on more complex systems. Note that this result is not in conflict with the discussion in the previous paragraph, because in a natural magma the presence of another crystalline phase or aluminum in enstatite could allow the reaction relation to take place even for a liquid composition undersaturated in silica.

Appendix

Contamination of Platinum Capsules by Silicon

For many years, users of piston-cylinder apparatus have noticed that platinum capsules melt far below the melting point of pure platinum (Boyd and England, 1963; Williams and Kennedy, 1969; Presnall *et al,* 1973), and it has generally been assumed that this is caused by contamination from the pressure cell. In some of our runs near the melting temperature of the capsule, we noticed an interesting texture in the capsule wall (Fig. 6). Electron microprobe study revealed that the texture consists of pure platinum crystals in a matrix of platinum-silicon alloy. The Pt-Si alloy contains only a small amount of Si, and no other elements were detected. An especially careful check was made for Al, Fe, and Mg.

The Pt-Si phase diagram (Hansen, 1958, p. 1140) shows a very steep liquidus curve descending from the melting point of pure Pt at 1769°C to a eutectic at 830°C, 23 mole percent Si, indicating that a small amount of silicon causes a dramatic reduction in the melting temperature. The texture in Figure 6 is a crystal-liquid mixture that has not quite reached the point of causing collapse of the crucible. The increasing width of the partially melted zone toward the inside of the capsule is a typical feature, and shows that the contamination originates from the sample itself, not from parts of the pressure cell outside the capsule.

For capsules that have not failed, loss of silicon from the sample is usually not significant. In our experience, failure of the capsule results when roughly 10–20 percent of the capsule develops the partially melted texture shown in Figure 6. Using these percentages, rough calculations indicate that the SiO_2 content of a sample would be reduced about 0.2-0.5 percent at the time of failure of the capsule. Most successful runs show capsules with far less than 10 percent development of the partial melting texture.

Presnall *et al* (1973) found that platinum capsules could be used at much higher temperatures and for longer runs when the capsule was completely encased by 99.7 percent Al_2O_3 ceramic rather than ceramics containing SiO_2. The explanation for this was not understood at the time, but it appears now that silicon is the external contaminant that accelerates melting of the capsule. Silicon contamination may also explain the very high drift rates of Pt/Pt10Rh thermocouples when they are used in the piston-cylinder apparatus in contact with mullite or Pyrex glass (Mao and Bell, 1971; Mao, Bell, and England, 1971).

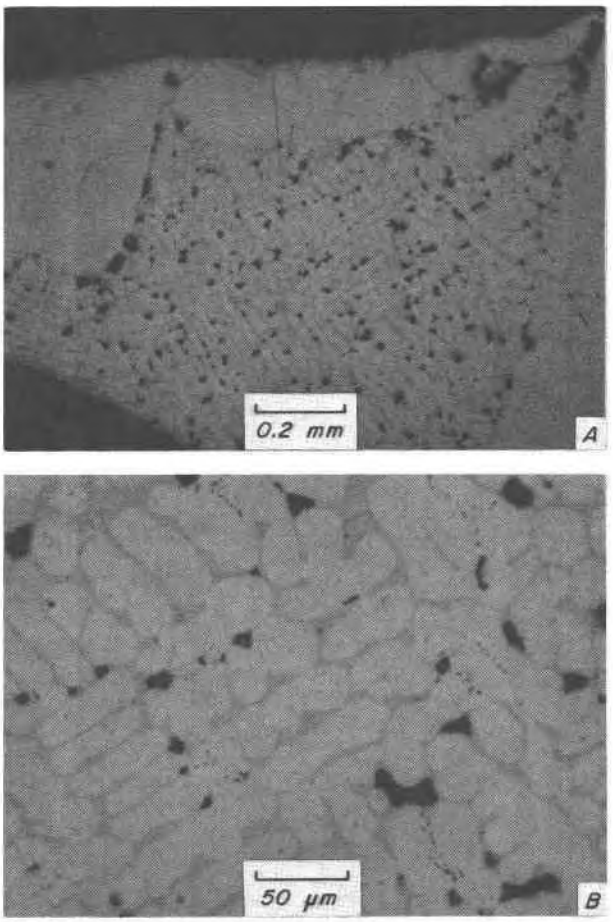

FIG. 6. Polished section of platinum capsule wall in reflected light showing partial melting texture. Light gray is Pt, medium gray is Pt-Si alloy, black spots are holes. In photograph A, the large black areas outline the margins of the capsule wall with the outside at the top. Run conditions were 1665°C, 7 kbar for 4 hrs.

Acknowledgments

We wish to thank G. V. Gibbs and D. H. Lindsley for critical reviews of the manuscript. This research was supported by the National Science Foundation, NSF Grant GA-21477.

References

ANASTASIOU, P., AND F. SEIFERT (1972) Solid solubility of Al_2O_3 in enstatite at high temperatures and 1-5 kb water pressure. *Contrib. Mineral. Petrol.* **34,** 272–287.

ANONYMOUS (1969) The international practical temperature scale of 1968. *Metrologia,* **5,** 35–44.

ATLAS, L. (1952) The polymorphism of $MgSiO_3$ and solid-state equilibria in the system $MgSiO_3$–$CaMgSi_2O_6$. *J. Geol.* **60,** 125–147.

BORG, I. Y., AND D. K. SMITH (1969) Calculated X-ray powder patterns for silicate minerals. *Geol. Soc. Am. Mem.* **122,** 896 pp.

BOWEN, N. L. (1928) *The Evolution of the Igneous Rocks.* Princeton University Press, Princeton, New Jersey, 332 p.

———, AND O. ANDERSEN (1914) The binary system MgO–SiO_2. *Am. J. Sci.* 4th ser. **37,** 487–500.

———, AND J. F. SCHAIRER (1935) The system MgO–FeO–SiO_2. *Am. J. Sci.* **29,** 151–217.

BOYD, F. R., AND J. L. ENGLAND (1960) Apparatus for phase-equilibrium measurements at pressures up to 50 kilobars and temperatures up to 1750°C. *J. Geophys. Res.* **65,** 741–748.

———, AND J. L. ENGLAND (1963) Effect of pressure on the melting of diopside, $CaMgSi_2O_6$, and albite, $NaAlSi_3O_8$, in the range up to 50 kilobars. *J. Geophys. Res.* **68,** 311–323.

———, ———, AND B. T. C. DAVIS (1964) Effects of pressure on the melting and polymorphism of enstatite, $MgSiO_3$. *J. Geophys. Res.* **69,** 2101–2109.

BUSECK, P. R., AND S. IIJIMA (1974) High resolution electron microscopy (HREM)—fine structures of enstatite. *Geol. Soc. Am. Abstr. Programs,* **6,** 676.

DAVIS, B. T. C., AND J. L. ENGLAND (1964) The melting of forsterite up to 50 kilobars. *J. Geophys. Res.* **69,** 1113–1116.

HANSEN, M. (1958) *Constitution of Binary Alloys,* 2nd ed. McGraw-Hill, New York, 1305 p.

KUNO, H. (1950) Petrology of Hakone volcano and the adjacent areas, Japan. *Geol. Soc. Am. Bull.* **61,** 957–1020.

KUSHIRO, I. (1968) Compositions of magmas formed by partial zone melting of the earth's upper mantle. *J. Geophys. Res.* **73,** 619–634.

———, H. S. YODER, JR. AND M. NISHIKAWA (1968) Effect of water on the melting of enstatite. *Geol. Soc. Am. Bull.* **79,** 1685–1692.

MAO, H. K., AND P. M. BELL (1971) Behavior of thermocouples in the single-stage piston-cylinder apparatus. *Carnegie Inst. Wash. Year Book,* **69,** 207–216.

———, ———, AND J. L. ENGLAND (1971) Tensional errors and drift of thermocouple electromotive force in the single-stage piston-cylinder apparatus. *Carnegie Inst. Wash. Year Book,* **70,** 281–287.

PRESNALL, D. C., N. L. BRENNER, AND T. H. O'DONNELL (1973) Drift of Pt/Pt10Rh and W3Re/W25Re thermocouples in single stage piston-cylinder apparatus. *Am. Mineral.* **58,** 771–777.

———, C. L. SIMMONS, AND H. PORATH (1972) Changes in electrical conductivity of a synthetic basalt during melting. *J. Geophys. Res.* **77,** 5665–5672.

RUCKLIDGE, J., AND E. L. GASPARRINI (1969) Electron microprobe analytical data reduction, EMPADR VII, Department of Geology, University of Toronto, Toronto, Canada (unpublished manuscript).

SMYTH, J. R. (1974) Experimental study on the polymorphism of enstatite. *Am. Mineral.* **59,** 345–352.

TAYLOR, H. C. J. (1973) Melting relations in the system MgO–Al_2O_3–SiO_2 at 15 kb. *Geol. Soc. Am. Bull.* **84,** 1335–1348.

TUTTLE, O. F., AND N. L. BOWEN (1958) Origin of granite in the light of experimental studies. *Geol. Soc. Am. Mem.* **74,** 153 p.

WILLIAMS, D. W., AND G. C. KENNEDY (1969) Melting curve of diopside to 50 kilobars. *J. Geophys. Res.* **74,** 4359–4366.

Manuscript received, September 30, 1974; accepted for publication, November 27, 1974.